4. (a) H. Münstedt, G. Köhler, H. Möhwald, D. Naegele, R. Bittihn, G. Ely, and E. Meissner, *Synth. Met.*, **18,** 259 (1987); (b) H. Münstedt and E. Voss, *Prog. Batt. Sol. Cells*, **6,** 250 (1987).
5. K. Imanishi, M. Satoh, Y. Yasuda, R. Tsushima, and S. Aoki, *J. Electroanal. Chem.*, **260,** 469 (1989).
6. P. Novák and W. Vielstich, *This Journal*, **137,** 1036 (1990).
7. K. Naoi, H. Sakai, S. Ogano, and T. Osaka, *J. Power Sources*, **20,** 237 (1987).
8. P. Novák, P. A. Christensen, T. Iwasita, and W. Vielstich, *J. Electroanal. Chem.*, **263,** 37 (1989).
9. (a) A. Bewick and K. Kunimatsu, *Surf. Sci.*, **101,** 131 (1980); (b) A. Bewick, K. Kunimatsu, and B. S. Pons, *Electrochim. Acta*, **25,** 465 (1980).
10. H. Neugebauer, A. Neckel, and N. Brinda-Konopik, *Springer Series in Solid-State Sciences*, **63,** 227 (1985).
11. P. A. Christensen, A. Hamnett, and A. R. Hillman, *J. Electroanal. Chem.*, **242,** 47 (1988).
12. (a) H. Neugebauer, A. Neckel, G. Nauer, N. Brinda-Konopik, F. Garnier, and G. Tourillon, *J. Physique, (Paris), Colloq. C-10*, **44,** 517 (1983); (b) H. Neugebauer, G. Nauer, A. Neckel, G. Tourillon, F. Garnier, and P. Lang, *J. Phys. Chem.*, **88,** 652 (1984); (c) N. S. Sariciftci, H. Neugebauer, H. Kuzmany, and A. Neckel, *Springer Series on Solid-State Sciences*, **76,** 228 (1987); (d) H. Neugebauer, N. S. Sariciftci, H. Kuzmany, and A. Neckel, *Mikrochim. Acta, (Wien)*, **1,** 265 (1988); (e) M. A. Habib and S. P. Maheswari, *This Journal*, **136,** 1050 (1989).
13. G. Eggert and J. Heitbaum, *Electrochim. Acta*, **31,** 1143 (1986).
14. (a) A. F. Diaz and J. I. Castillo, *J. Chem. Soc. Chem. Commun.*, 397 (1980); (b) F. Trinidad, J. Alonso-Lopez, and M. Nebot, *J. Appl. Electrochem.*, **17,** 215 (1987).
15. G. Socrates, "Infrared Characteristic Group Frequencies," p. 57, 98, and 144, Wiley, Chichester (1980).
16. "Sadtler Standard Spectra, IR Grating," Sadtler Research Laboratories, Inc., Philadelphia, PA; (a) spectrum No. 376 K (1966), (b) spectrum No. 29556 K (1973).
17. R. J. Waltman and J. Bargon, *Tetrahedron*, **40,** 3963 (1984).
18. G. B. Street, in "Handbook of Conducting Polymers," Vol. 1, T. A. Skotheim, Editor, p. 280, Marcel Dekker, New York and Basel (1986).
19. S. I. Yaniger and D. W. Vidrine, *Appl. Spectros.*, **40,** 174 (1986).
20. J. Heinze and M. Dietrich, *Materials Science Forum*, **42,** 63 (1989).
21. (a) F. Beck, M. Oberst, and P. Braun, *Dechema-Monographien*, **109,** 457 (1987); (b) F. Beck and M. Oberst, *Makromol. Chem., Macromol. Symp.*, **8,** 97 (1987); (c) J. Heinze, M. Dietrich, and J. Mortensen, *ibid.*, **8,** 73 (1987).
22. F. Beck, *Electrochim. Acta*, **33,** 839 (1988).
23. S. Panero, P. Prosperi, and B. Scrosati, *ibid.*, **32,** 1465 (1987).

Application of the Boundary-Element Method to Offshore Cathodic Protection Modeling

P. Cicognani

Snamprogetti SpA, 61032 Fano (PS), Italy

F. Gasparoni

Tecnomare SpA, 30124 Venezia, Italy

B. Mazza and T. Pastore

Dipartimento di Chimica Fisica Applicata, Politecnico di Milano, 20133 Milano, Italy

ABSTRACT

This paper deals with the main aspects of the calculation of current and potential distributions and summarizes some results obtained on different systems using a computer program based on the boundary-element method. Model results are compared to literature data for well-known geometries, and to experimental data obtained both in laboratory testing with a suitable cell and in field testing on offshore structures (in particular platform nodes). The good predictive capability of computer modeling is shown.

Offshore steel structures are protected against corrosion by means of cathodic protection systems. Cathodic protection design should guarantee an adequate current and potential distribution on the structure surface throughout the whole structure lifetime. Insufficient protection levels can lead to dangerous corrosion phenomena on important parts of the structure, requiring the retrofitting of the cathodic protection system. This would involve far greater costs than those required to set up an efficient protection system on the stocks, on account of subsea operations. Conversely, an excessively conservative approach can give rise to overprotection levels. Moreover, in case of sacrificial anode protection systems and particularly on the platforms that are being built for deep-water operations, this approach can increase structure loading, due to the greater anode weight and to the higher structure resistance to sea motion.

On the other hand, traditional design methods are based on the use of average values of protection current density, and ignore the problem of calculating current and potential distribution; this is left to the engineer's experience in distributing the anodes on the structure. These methods are therefore unable to guarantee the efficiency of the protection on complex structures and in all cases where no previous experience has been acquired.

The calculation of current and potential distribution is today considered an indispensable means of general development for cathodic protection systems and for the study and improvement of their reliability. Today, the calculation of distribution on such complex structures as offshore platforms is made possible by numerical techniques. The finite element method (FEM), the finite difference method (FDM), and, more recently, the boundary-element method (BEM), introduced long since in other fields, have proved

to be applicable (1-5).[1] But the calculation of distribution also requires the ability to describe quantitatively the phenomena occurring on the surface of the protected structure (boundary condition equations). In this regard, more larger knowledge is required and is now considered indispensable for general development of cathodic protection.

These considerations led Agip, Snamprogetti, and Tecnomare, in cooperation with the Politecnico di Milano, to carry out a joint research project aimed at developing a computer program for cathodic protection modeling in case of offshore structures. This project, financed by IMI (Istituto Mobiliare Italiano), started in 1984 and ended in 1987. The calculation program setup is based on the boundary-element method (BEASY equation solver[2]) and is able:[3]

i.) To carry out two-dimensional analysis.
ii.) To carry out global three-dimensional analysis of tubular structures (*e.g.* platform jackets).
iii.) To perform local three-dimensional analysis of selected parts of the structure (*e.g.*, platform nodes).
iv.) To analyze cathodic protection systems either using sacrificial anodes or impressed current.
v.) To solve problems of primary, secondary, and tertiary distribution.
vi.) To handle time-dependent boundary conditions.

The main objective of this paper is to prove the good predictive capability of computer modeling. In order to do that, model results are compared to:

i.) Literature data for well-known geometries.
ii.) Experimental data obtained in laboratory testing with a suitable cell.
iii.) Experimental data obtained in field testing on offshore structures (in particular platform nodes).

Laboratory testing was conducted at the Politecnico di Milano. Field testing refers to a survey performed by Corrocean on two of Agip's platforms located in the Adriatic Sea, BASIL, and PCW-A. Computer analyses were developed by Tecnomare and Snamprogetti.

Background

Under the conditions that concentration gradients are negligible inside the electrolytic solution and the diffusion layer is of negligible thickness compared to the system dimensions, the distribution of potential (ϕ) can be obtained by solving Laplace's equation

$$\text{div grad } \phi = 0 \qquad [1]$$

while the current distribution satisfies the relationship between current density (i) and potential gradient (Ohm's law)

$$i = -K \text{ grad } \phi \qquad [2]$$

(where K is the specific conductivity of the electrolytic solution).

On the structure surface to be protected (cathode) and on the anodes, boundary conditions for the integration of Laplace's equation correspond to the polarization curves of the materials. As a matter of fact, the current density exchanged at an electrode surface is a function of the overpotential (η) according to the kinetic equation

$$i = f(\eta) \qquad [3]$$

and the potential at the solution side of the electrode-solution interface is linked with overpotential by the relationship

$$\phi = \text{const} - \eta \qquad [4]$$

the electrode being equipotential.

On the anodes, simplified boundary conditions are generally assumed, being close to actual conditions; for sacrificial anodes (made of zinc or aluminum) a constant potential is taken, *i.e.*, such anodes are considered as unpolarizable, whereas in impressed current systems the current output from each anode is obviously imposed.

Steel polarization curve.—The cathodic behavior in seawater of carbon and low alloy steels is described by the continuous curve shown in Fig. 1. In first approximation, it can be assumed that the steel polarization curve results from three processes:

i.) Anodic reaction of iron dissolution

$$Fe = Fe^{2+} + 2e^- \qquad [5]$$

ii.) Cathodic process of oxygen reduction

$$2H_2O + O_2 + 4e^- = 4\ OH^- \qquad [6]$$

iii.) Cathodic process of hydrogen evolution

$$2H_2O + 2e^- = H_2 + 2\ OH^- \qquad [7]$$

At potential values involved in cathodic protection, around −800 mV *vs.* standard calomel electrode (SCE), the cathodic process of oxygen reduction takes place under limiting current conditions; its rate can therefore be represented by a constant term, regardless of potential (i_l).

The process of hydrogen evolution prevails at more negative potentials, *i.e.*, in the presence of cathodic overprotection; it starts to be evident at potential values around −1000 mV *vs.* SCE. At more positive potentials, exceeding the free corrosion potential value, the anodic process of iron dissolution prevails, whereas below that value, the anodic process rate decreases with the potential until it becomes negligible at the protection potential value (−800 mV *vs.* SCE). The kinetic Eq. [3] for both the anodic iron dissolution and the cathodic hydrogen evolution processes can be described by an exponential relationship (Tafel's law). The overall polarization curve, *i.e.*, the boundary conditions on the steel structure, can be expressed by the following equation

$$i = I_{Fe} \exp(E/B_{Fe}) - i_l - I_H \exp(-E/B_H) \qquad [8]$$

(where i is the current density exchanged at the electrode surface [anodic if it is positive and cathodic if negative] and

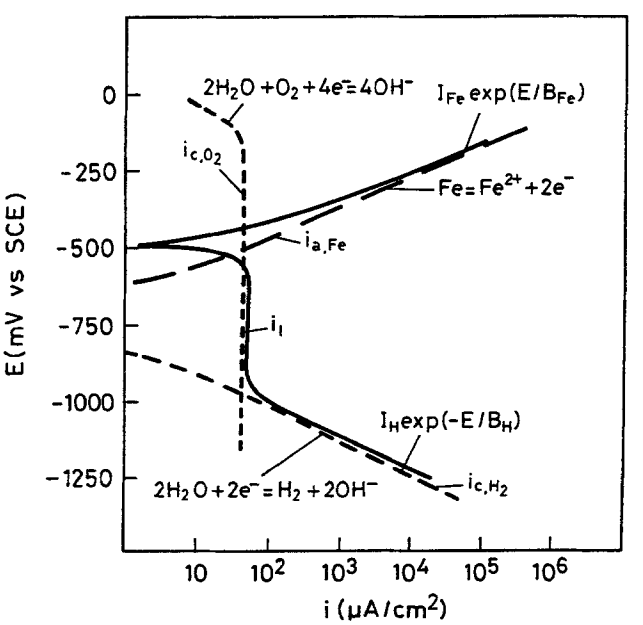

Fig. 1. Schematic polarization curve (solid line) and partial reactions for steel in seawater.

[1] The three different methods of numerical calculation used for the determination of current and potential distribution present different problems. However, the BEM method is considered to be the most efficient in the case of cathodic protection systems. Without dealing with mathematical aspects, this method has the advantage of solving field equations only on the surface of the structure, that is, only in the zones where current and potential distribution need to be calculated. Moreover, as surface elements can be either plane or curved, difficulties in the discretization are much reduced and the mathematical representation of the structure can be more easily carried out.

[2] In this connection, the success of other models, such as that developed by Conoco based on the BEASY program, should also be acknowledged (4, 5).

[3] Due to their particular characteristics, different types of boundary elements are used in the various situations listed below. Mainly, they are: linear elements for two-dimensional analysis, and tubular and quadrilateral elements for three-dimensional analysis.

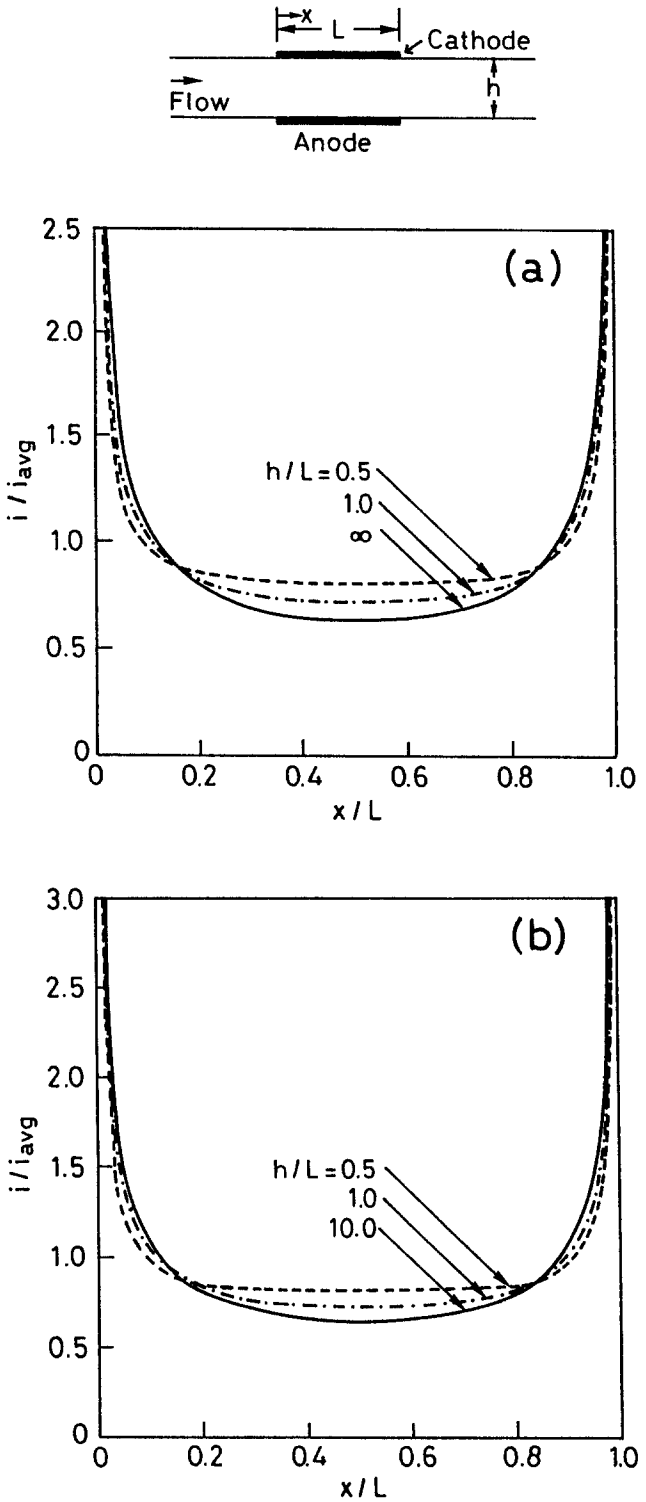

Fig. 2. Parallel plate electrodes in a flow channel: a) analytical solution of the primary current distribution (12); b) calculated primary current distribution. Subscript avg stands for average. Conductivity of electrolyte assumed 1 Ω^{-1} m^{-1}.

E is the electrode potential). The five parameters required for the above-cited expression (I_{Fe}, B_{Fe}, i_l, I_H, B_H) can be easily obtained from the experimental polarization curve, as shown in Fig. 1.

In the literature (6-8), other expressions are reported for the steel polarization curve that are substantially equivalent to that reported above. Although carbon's and low alloy steel's behavior in a marine environment is well known, the quantitative description of the polarization curve presents some important problems (9). The factors affecting the polarization curve and the amount of current exchanged at a given electrode potential value are numerous and mutually dependent. They can be divided into factors due to the structure and factors connected to the marine environment.

The former group includes: *i.*) Superficial state of the steel of the structure (presence of mill scale or of oxides due to previous corrosion); and *ii.*) geometrical characteristics of the structure.

The latter group includes: *i.*) oxygen concentration in water; *ii.*) water motion and presence of solids in suspension; *iii.*) formation of calcareous deposit; *iv.*) marine fouling; *v.*) salinity; and *vi.*) temperature.

The maximum amount of oxygen that can reach the cathodic surface of the structure in a given time (and therefore the i_l value) is determined by the oxygen concentration in water and by the transport mechanism towards the surface of the structure itself. In absence of superficial deposits on the metal, this transport is essentially of convective type and is due to sea motion, in relation to the geometrical characteristics of the structure. The oxygen transport to metal can be hampered by fouling, by the presence of corrosion products, by the formation of a calcareous deposit. This is formed on the cathode in consequence of the *p*H increase due to the reactions that occurred. Rough sea conditions and suspended solids can abrade the surface of the structure and hamper the formation of the calcareous deposit or destroy it and therefore demand an increase in the current necessary to protect the structure.

Temperature has an influence on the oxygen solubility as well as on oxygen diffusion rate, on the parameters affecting oxygen convective transport, on fouling growth, on the oxygen exchange between sea and atmosphere (which is also affected by sea state), and on the growth of marine organisms that also contribute to determining the content of dissolved oxygen (photosynthesis, etc.).

The growth of the calcareous deposit is affected, not only by temperature, but also by the value of cathodic current density, by hydrodynamic conditions, and by seawater chemical properties. The hydrogen evolution takes place at a different rate on the metal surface covered by oxides rather than mill scale; the presence of a non-conductive superficial deposit (calcareous deposit) can reduce the reaction rate. Also, the reaction rate is a function of the chemical properties of the environment and of temperature. The same applies to the anodic process of iron disso-

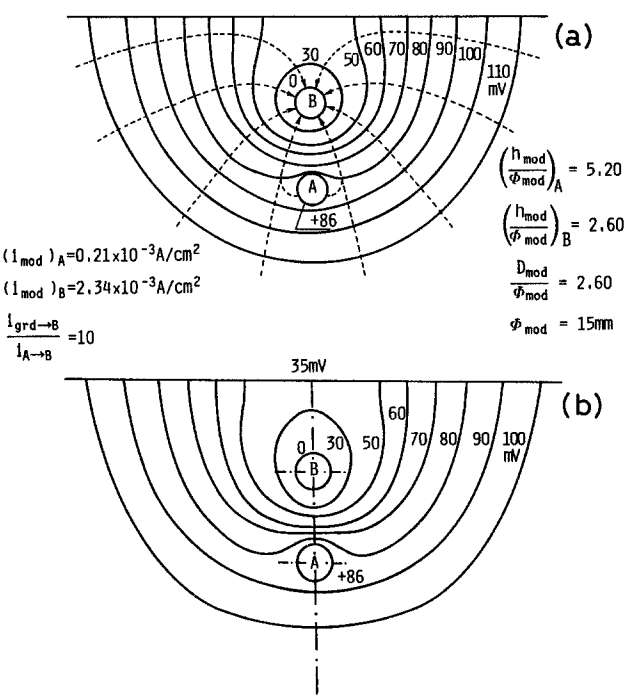

Fig. 3. Buried pipeline electrochemical model applied to the study of interference phenomena: a) experimental isopotential lines (11); b) computed iso-potential lines in primary distribution. Conductivity of electrolyte 5.392 Ω^{-1} m^{-1}. ϕ = pipeline diameter; h = depth of burial; D = distance between axes of two parallel pipelines A and B; subscript mod stands for model; subscript grd stands for ground.

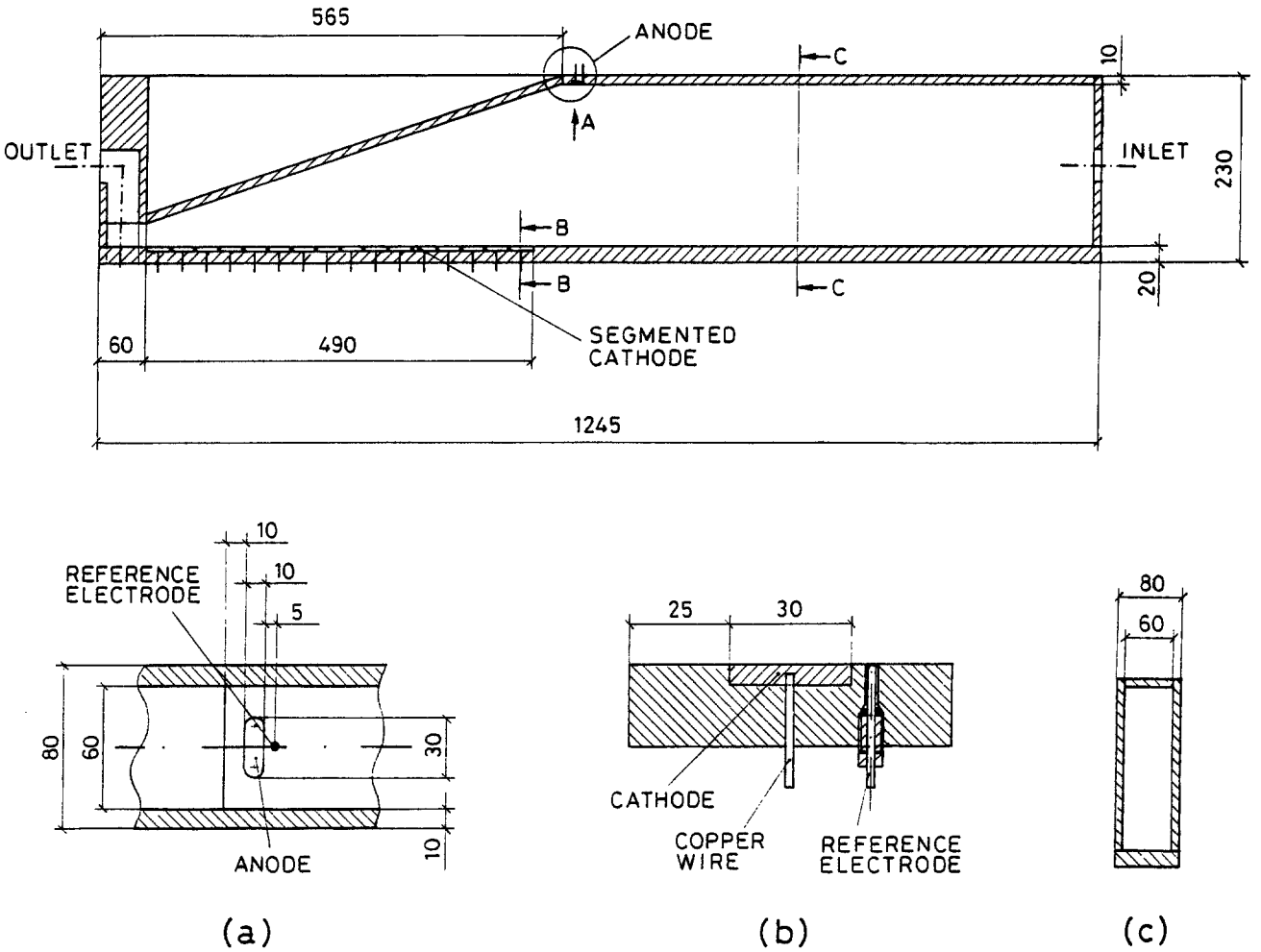

Fig. 4. Cell with segmented cathode for experimental testing of the calculation program: horizontal section and other views. a) Detail A, view in direction of arrow; b) B-B sectional view; c) C-C sectional view. Sizes are in mm.

lution; particularly, corrosion products slow down both iron dissolution and the oxygen reduction cathodic process. Adherent and conductive oxides, such as mill scale, can prevent the dissolution of underlying steel, though causing localized corrosion on unprotected areas.

In conclusion, polarization curves in seawater can vary depending on the geographical site, time, depth, and geometrical characteristics of the structure. The definition of boundary conditions on real structures can only be coped with by means of systematic studies of the main factors (*i.e.*, growth of the calcareous deposit) and through new techniques of surveying able to provide information on the location where the structure to be protected is or has to be built. Laboratory studies have to set up models capable of utilizing available data and to provide a mathematical definition of boundary conditions. Despite the complexity of the phenomena involved, Eq. [8], reported above for boundary conditions on a carbon or low alloy steel offshore structure, can be considered formally valid, provided that a correct estimate of parameters is done.

Applications of the Model

The calculation program for current and potential distribution was applied to various geometries, reported in Table I. Several cases were examined, either with primary distribution (10-13), or secondary distribution and linear polarization curve (12, 13), or tertiary distribution (14-16). In order to determine program accuracy, calculated distributions were compared either to available literature data (10-13), or to experimental data collected in the present research project (14-16). Figures 2 through 7 show current and potential distributions for some of the systems studied.

The sequence of the different cases corresponds to the chronological order of the various phases of the research project (bibliographical review, laboratory testing, field testing). At the same time, it is connected to an ever increasing complexity of the systems, from both a geometrical and an electrochemical point of view, and consequently to an ever more sophisticated development of calculation systems required. Figure 2 reports the results obtained on a channel flow cell having plane, parallel electrodes, in the case of primary distribution. For this case, the analytical solution is given by Parrish and Newman (12).

Figure 3 shows the results (still in the case of primary distribution) of a two-dimensional analysis of the system used by Bianchi (11) to study interference phenomena on buried pipelines (gas pipelines). Comparison data were obtained by Bianchi on a laboratory cell with appropriate electrodes and electrolytic solution (lead in lead sulfamate solution) where distribution was primary. Besides the case shown in Fig. 3, other cases studied by Bianchi have been analyzed, always obtaining results very close to laboratory data. In particular, the distribution was solved in the case of laboratory electrochemical models used by Bianchi to study the effects of the depth of burial, of the presence of an insulating coating on the pipeline, and of the interference between two neighboring pipelines.

A three-dimensional analysis was performed on the cell of Fig. 4 set up to study the influence of hydrodynamic conditions in cathodic protection systems (in this cell a 3.5% NaCl solution circulated through an external flow system). Tertiary distribution was considered and boundary conditions were expressed by the above-reported Eq. [8], assuming for the parameters I_{Fe}, B_{Fe}, I_H, and B_H the values reported in literature by Turnbull and Gardner (17).[4] The limiting current density for oxygen reduction

[4] $I_{Fe} = 1.5 \times 10^7$ A/cm^2, $B_{Fe} = RT/F = 25.3$ mV, $I_H = 8 \times 10^{-14}$ A/cm^2, $B_H = 2\ RT/F = 50.6$ mV (i is in A/cm^2 and E in mV *vs.* SCE).

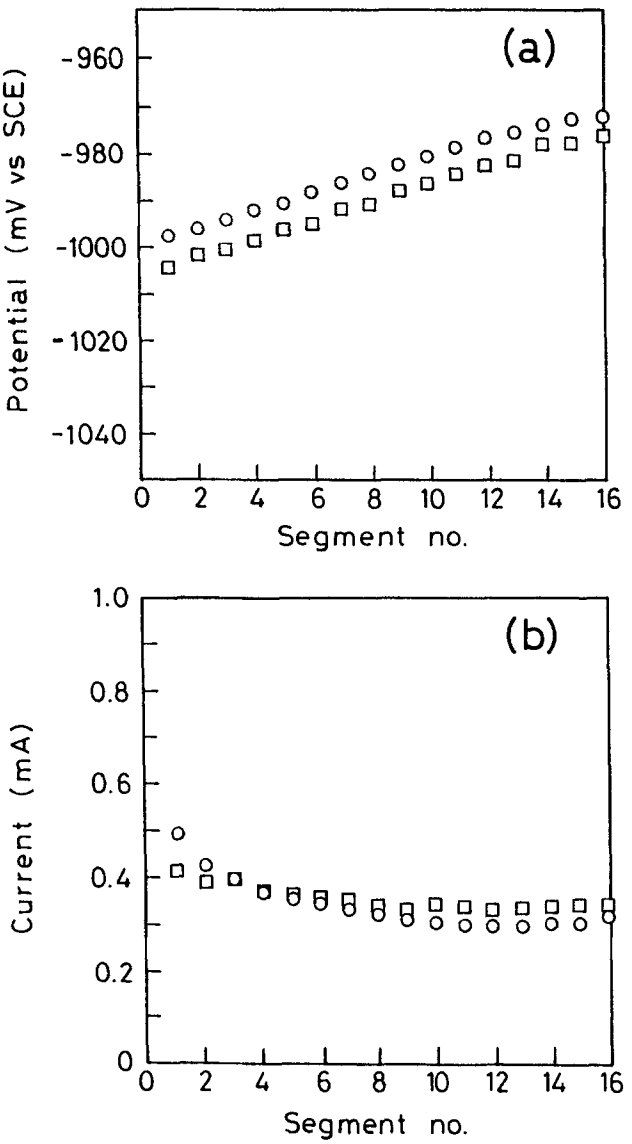

Fig. 5. Potential (a) and current (b) distributions on the segmented cathode of the cell shown in Fig. 4. Segments are numbered so that segment number 1 is the closest to the anode and segment number 16 is the farthest away. Sacrificial anode cathodic protection system. Type of anode: zinc alloy. Solution flow rate: 110 1/h. Squares stand for experimental; circles stand for calculated in tertiary distribution. Limiting current density obtained following correlation [9]. Conductivity of solution 5.02 Ω^{-1} m^{-1}.

was obtained in two different ways (14): either starting from the theoretical correlation valid for laminar flow between parallel plate electrodes (18-21), merely modified for cell geometry,[5] or (with better accuracy) using a semi-empirical correlation obtained from suitable tests[6]. Potential and current distribution in case of solution flow rate of 110 1/h is reported in Fig. 5. Model accuracy in the case of three-dimensional analysis and tertiary distribution is still satisfactory.[7]

$$i_l = 1.2325\, n\mathbf{F}CD^{2/3}V^{1/3}\,(h + y/2h^2y^2x)^{1/3} \qquad [9]$$

(where n is the equivalent per mole, $\mathbf{F}$ is Faraday's constant (C/equiv), C is the concentration of dissolved O_2 (mol/cm^3), D is the diffusion coefficient of dissolved O_2 (cm^2/s), V is the volumetric flow rate (cm^3/s), x is the distance along the cathode (cm), y is the cell width (cm), h is the cell height (cm), and i_l is in A/cm^2).

$$i_l = 2.3\, n\, \mathbf{F}CD^{2/3}\,(V/x)^{1/3}\,(1/hy)^{1/2} \qquad [10]$$

In the presence of turbulent flow, this correlation is not able to make a correct estimate of the limiting current density either (see Table I, footnote g).

[7] The considerable error (about 100 mV) found during one of the tests reported in Table I (see footnote h) is mainly (at least 80 mV) due to an error in assuming the value of parameter I_{Fe}. In fact, Turnbull and Gardner data have been obtained in de-aerated NaCl solutions, whereas in an aerated environment some passivation phenomena take place (22).

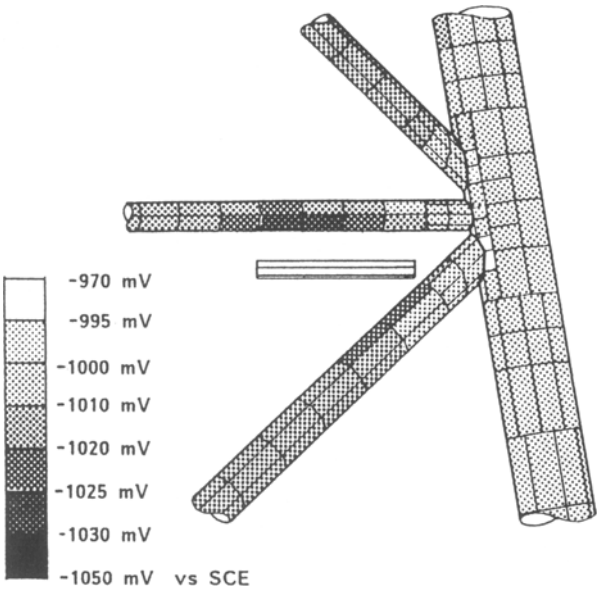

Fig. 6. Three-dimensional local analysis of potential distribution on a node of BASIL platform with sacrificial anode cathodic protection system. Type of anode: aluminum alloy. Tertiary distribution. Boundary conditions on the structure: see text. Conductivity of seawater 4.21 Ω^{-1} m^{-1}. Platform leg diameter 1150 mm; horizontal brace diameter 406 mm; upward diagonal brace diameter 558 mm; downward diagonal brace diameter 609 mm. Anode length 2450 mm. Distance from structure surface to anode: approx. 350 mm.

Figure 6 and 7 report the potential distribution calculated on a node of the Agip's BASIL platform. The distribution on such a complex structure had to be calculated in successive step. First, the distribution on the whole structure discretized in macroelements (tubular elements[8]) was determined, then a more detailed analysis was locally carried out,[9] starting from the general distribution calculated

[8] Which model straight cylindrical voids of constant radius well. With tubular elements, the problem variables (potential and current) must remain uniform around the tube and may vary only along the axis.

[9] The discretization of the node was performed using an interactive meshing program. In this step, to follow the true shape of the detail of interest, quadrilateral surface elements with constant shape functions are used. This means that the results are computed in a single node inside the element with the approximation that the problem variables are considered constant over the whole element surface.

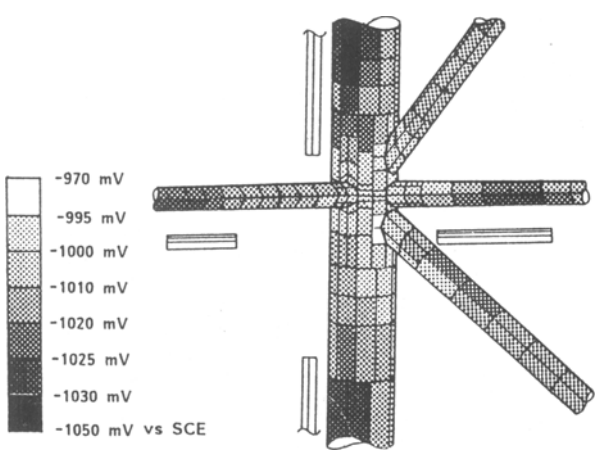

Fig. 7. Three-dimensional local analysis of potential distribution on a node of BASIL platform with sacrificial anode cathodic protection system (a different angle slot of the same node shown in Fig. 6). Type of anode: aluminum alloy. Tertiary distribution. Boundary conditions on the structure: see text. Conductivity of seawater 4.21 Ω^{-1} m^{-1}. Platform leg diameter 1150 mm; horizontal braces diameter 406 mm; upward diagonal brace diameter 558 mm; downward diagonal brace diameter 609 mm. Anode lengths 2450 and 1750 mm. Distance from structure surface to anode: approx. 350 mm.

Table I. Summary of cases analyzed

System analyzed	Type of analysis	Type of distribution	Average error in potential	Average error in current	Comparison data used
Concentric spherical electrodes	Axisymmetric	Primary	<0.2%[a]	<0.5%	Analytical solution
Concentric cylindical electrodes	Axisymmetric	Primary	0.1%[a]	<0.2%	Analytical solution
Slot-electrode cell	Two-dimensional	Primary	—[b]	<8%	Other computer solution (10) (Schwarz-Christoffel transformation)
Buried pipeline electrochemical model	Two-dimensional	Primary	10%	—[c]	Experimental data (11) (laboratory testing)
Parallel-plate electrodes in a flow channel	Two-dimensional	Primary	—[c]	3%	Analytical solution (12) Other computer solution (13) (FDM method)
Parallel-plate electrodes in a flow channel	Two-dimensional	Secondary linear polarization	—[c]	7%	Numerical solution (12) Other computer solution (13) (FDM method)
Cell of Fig. 4, with electrolyte circulation. Sacrificial anode CP[d] system Flow rate 500 1/h	Three-dimensional	Tertiary[e]	3.6 mV	13%	Experimental data (14) (laboratory testing)
Cell of Fig. 4, ditto Flow rate 200 1/h	Three-dimensional	Tertiary[e]	5.3 mV	12%	Experimental data (14) (laboratory testing)
Cell of Fig. 4, ditto Flow rate 100 1/h	Three-dimensional	Tertiary[e]	13.6 mV	14%	Experimental data (14) (laboratory testing)
Cell of Fig. 4, ditto Flow rate 110 1/h	Three-dimensional	Tertiary[e]	5.6 mV	8%	Experimental data (14) (laboratory testing)
Cell of Fig. 4, ditto Flow rate 1000 1/h	Three-dimensional	Tertiary[f]	17.2 mV	5%	Experimental data (14) (laboratory testing)
Cell of Fig. 4, ditto Flow rate 2000 1/h	Three-dimensional	Tertiary[f]	31.3 mV	30%[g]	Experimental data (14) (laboratory testing)
Cell of Fig. 4, with electrolyte circulation Impressed current CP[d] system Flow rate 500 1/h Current 5.2 mA	Three-dimensional	Tertiary[f]	97.3 mV[h]	12%	Experimental data (14) (laboratory testing)
Cell of Fig. 4, ditto Current 6 mA	Three-dimensional	Tertiary[e]	74.2 mV	8%	Experimental data (14) (laboratory testing)
Cell of Fig. 4, ditto Current 8 mA	Three-dimensional	Tertiary[e]	33.1 mV	5%	Experimental data (14) (laboratory testing)
BASIL platform Sacrificial anode CP[d] system	Three-dimensional Global	Tertiary	20 mV	15%	Experimental data (15, 16) (field testing)
BASIL platform node	Three-dimensional Local	Tertiary	10 mV	20%	Experimental data (15, 16) (field testing)
PCW-A, platform Impressed current CP[d] system	Three-dimensional Global	Tertiary	100 mV[i]	50%[i]	Experimental data (15, 16) (field testing)
PCW-A, platform node	Three-dimensional Local	Tertiary	30 mV	25%	Experimental data (15, 16) (field testing)

[a] With reference to the values in some points selected inside.
[b] Potential is given.
[c] Comparison data not reported.
[d] Cathodic protection.
[e] Limiting current density obtained following correlation [9].
[f] Limiting current density obtained following correlation [10].
[g] Error due to presence of turbulent flow.
[h] An error of about 80 mV in the estimate of the steel anodic polarization curve is included.
[i] Error due to current unbalance in the calculation model.

in the previous step. As to the boundary conditions to assign to sacrificial anodes (made of an aluminum alloy) placed on the BASIL platform, a constant potential value of −1050 mV *vs.* SCE was assumed (equal to the specification value). In the case of an impressed current protection system on the PCW-A platform, the value of the current output read on the platform was assumed equal to 140A. The determination of boundary conditions on the structure represented the most delicate problem. No literature data were available for estimating the five parameters used for the expression [8] of boundary conditions. Available data applied to bare metal, *i.e.*, to sand-blasted or pickled steel, whereas the platforms were immersed in seawater and cathodically protected for a long time; therefore the jacket surface was covered by a layer of fouling and calcareous deposit. A model was set up to determine the effect of the calcareous deposit growth on the polarization curve (9, 23). Based on this model, the reduction in values of I_{Fe} and I_H parameters was evaluated with respect to the values for bare steel.[10] Limiting current density for oxygen reduction was estimated based on measurements performed *in situ*.[11]

Discussion

The results obtained proved that the calculation model generally matches comparison values. In the case of primary distribution, high accuracy is obtained and depends on how the structure has been discretized. In the case of secondary and tertiary distribution, accuracy still depends on the type of discretization adopted, but is largely affected by the reliability of boundary conditions and by the availability of useful data. For the cases studied in the laboratory, with environmental parameters sufficiently well-known and/or under relatively simple conditions (com-

[10] A reduction factor of 10 was assumed.

[11] It was chosen to be equal to 10^{-6} A/cm^2 in the case of the BASIL platform and equal to 2×10^{-6} A/cm^2 in the case of the PCW-A platform.

pared to actual conditions in a marine environment), the difference between calculated values and experimental data is less than 15% for current density and less than 30 mV for potential. In tests carried out on offshore structures, such differences for current density rise up to 20-25%; however, it has to be considered that boundary conditions were estimated based on field data, but were interpreted according to models still under study.

Two critical points should be underlined in the whole procedure. The first critical point is of a mathematical nature and deals with the need to provide the equation solver with a geometrical representation that best meets its peculiar requirements. It was observed that a correct modeling of the geometry of the system under study (including the choice of the number and dimensions of the various elements, the choice of the number and the shape of the zones in which the system is supposed to be subdivided, and the choice of the shape functions) guarantees that results would be free from numerical errors introduced by calculation. This point is intrinsic to the nature of the BEASY equation solver; therefore the only way to avoid errors in the result is to carefully prepare the modeling of the system's geometry. The quality of the mathematical representation was indicated by the unbalance between anodic and cathodic currents: the less accurate the modeling, the greater the unbalance, and therefore the worse the quality of results.[12,13]

The second critical point to be stressed is strictly connected to the nature of the problem that the equation solver is dedicated to handling: it concerns the large influence exerted by the estimate of oxygen-limiting current density on results. In the tertiary distribution cases examined, it was observed that the more accurate the results obtained, the more accurate the estimate of oxygen-limiting current density. This dependence is very strong in the potential range most widely used in cathodic protection (−750 to −950 mV *vs.* SCE) and can cause rough errors (up to 300 mV on potential) if the estimate is not accurate. This is mainly due to the particular shape of the polarization curve of steel in seawater. This curve shows an almost vertical trend (practically at constant current density) in its section of greater interest. In order to guarantee reliable results, it is therefore necessary to provide the equation solver with the most accurate possible boundary conditions. A correct estimate of boundary condition [8] parameters is extremely difficult in the case of platforms, as they are not only affected by fluidodynamic conditions, but also by the formation of calcareous deposit.

Conclusions

Computer solutions obtained for current and potential distribution prove the calculation program accuracy for various geometrical configurations, in the presence of primary, secondary, and tertiary control. The major problem is now the estimate of boundary conditions. Systematic studies have to be carried out on the various phenomena occurring on the surface of the cathodically protected offshore structures and suitable models have to be set up, in order to interpret data measured *in situ*. The good predictive capability of the computer program makes it applicable in analyzing existing cathodic protection systems in a marine environment, and this surely represents a first step towards advanced design methods for cathodic protection systems.

[12] In the case of the cell shown in Fig. 4, at the end of several attempts made to find out the best subdivision, the unbalance, which initially was 18%, was reduced to an acceptable figure of 5%, then remained constant throughout all the tests performed on this system, as a proof of its exclusive dependence on the type of geometrical modeling.

[13] The major difference between comparison (experimental) data and those obtained from the global analysis of the jacket of the PCW-A platform (see Table I, footnote i) is due to the inadequacy of the type of discretization adopted.

Acknowledgments

The authors wish to gratefully acknowledge the cooperation of R. Basana and E. Ferrari.

Manuscript submitted Dec. 28, 1988; revised manuscript received Jan. 24, 1990.

The Dipartimento di Chimica Fisica Applicata, Politecnico di Milano, assisted in meeting the publication costs of this article.

REFERENCES

1. E. A. Decarlo, *Mater. Perform.*, **22,** (7), 38 (1983).
2. R. Strommen and A. Rodland, *ibid.*, **20,** (4), 15 (1981).
3. J. W. Fu and J. S. K. Chow, *ibid.*, **21,** (10), 9 (1982).
4. R. Strommen, W. Keim, J. Finnegan, and P. Mehdizadeh, *ibid.*, **26,** (2), 23 (1987).
5. R. Strommen, in "U.K. Corrosion '86," Vol. 1, p. 183 Institution of Corrosion Science and Technology, Birmingham, England (1986).
6. O. F. Devereux, *Corrosion (Houston)*, **35,** 125 (1979).
7. Y. Massiani, J. P. Crousier, J. Crousier, J. Galea, and R. Romanetti, *Electrochim. Acta*, **29,** 1679 (1984).
8. R. S. Munn, *Mater. Perform.*, **21,** (8), 29 (1982).
9. T. Pastore, Tesi di Dottorato di Ricerca, Politecnico di Milano, Milano, Italy (1989).
10. M. E. Orazem and J. Newman, *This Journal*, **131,** 2857 (1984).
11. G. Bianchi, "Il problema della protezione dei metanodotti dal punto di vista della protezione elettrolitica," Stazione Sperimentale per i Combustibili, Milano, Italy (1955).
12. W. R. Parrish and J. Newman, *This Journal*, **117,** 43 (1970).
13. U. Landau and W. J. Cook, SBIR Phase I Final Report, Contract No. DE-AC01-83ER80064, U.S. Department of Energy, Washington, D.C. (1984).
14. B. Mazza, T. Pastore, P. Pedeferri, G. Taccani, E. Ferrari, and F. Gasparoni, in Proc. 10th International Congress on Metallic Corrosion, Vol. 2, p. 945, Oxford and IBH Publishing Co. Pvt. Ltd., New Delhi, India (1987).
15. F. Gasparoni, Rapporto finale Tecnomare No. 623057-REL-C830-T037, Venezia, Italy (1987).
16. I. H. Hollen, "Agip CP/CD Study—Survey of the BASIL and the PCW-A Platforms," Corrocean Report, Trondheim, Norway (1986).
17. A. Turnbull and M. K. Gardner, *Corros. Sci.*, **22,** 661 (1982).
18. U. Landau, in AIChE Symposium Series, No. 204, Vol. 77, p. 75 (1981).
19. J. R. Selman and C. W. Tobias, in "Advances in Chemical Engineering," Vol. 10, p. 211, Academic Press, New York (1978).
20. D. J. Pickett and B. R. Stanmore, *J. Appl. Electrochem.*, **2,** 151 (1972).
21. J. Newman, *Ind. Eng. Chem.*, **60,** 12 (1968).
22. B. Mazza, T. Pastore, P. Pedeferri, and G. Rondelli, in Proc. 10th International Congress on Metallic Corrosion, Vol. 1, p. 501, Oxford and IBH Publishing Co. Pvt. Ltd., New Delhi, India (1987).
23. R. Basana, F. Gasparoni, and T. Pastore, in "Proc. Convegno Corrosione Marina," AIM, Milano, Italy (1988).